Density and Potential Fluctuation Measurements in the Tandem Mirror GAMMA 10 Plasma

Masayuki YOSHIKAWA, Yoshiaki MIYATA, Toshiaki MATSUMOTO, Masanori MIZUGUCHI, Yoshitaka YONEDA, Shinsuke NEGISHI, Neo IMAI, Kazutaka KIMURA, Yoriko SHIMA, Youhei OONO, Akiyosi ITAKURA, Hitoshi HOJO, and Tsuyoshi IMAI

Plasma Research Center, University of Tsukuba, Tsukuba, Ibaraki 305-8577, Japan

(Received: 29 August 2008 / Accepted: 13 November 2008)

We observed the suppressions of density fluctuations by the potential formation during electron cyclotron heating (ECH) in the GAMMA 10 tandem mirror plasma. In the radial positions where electric field gradient is lower region, the density fluctuation powers are larger than those in the other positions. Moreover, we observed the suppression of the potential fluctuation during the confining potential formation by ECH. The density and potential fluctuations are observed by using the multichannel interferometer and gold neutral beam probe system (GNBP), respectively. Then, we can study more detail about plasma confinement during the formation of confinement potential produced by ECH.

Keywords: GAMMA 10, density fluctuation, potential fluctuation, the multichannel microwave interferometer, the gold neutral beam probe system

1. Introduction

The study of turbulent fluctuations in magnetic confinement system is very important for improving the plasma confinements. Various theories predict such turbulent fluctuations lead to anomalous transport and energy loss in the transverse direction. Low frequency plasma turbulence and the resultant anomalous transport observed in various devices exhibit rather common features [1,2]. In the tandem mirror GAMMA 10, the plasma confinement is achieved by not only a magnetic mirror configuration but also high potentials at the both end regions [3-11]. We have constructed a multi-channel microwave interferometer in order to measure the electron density and density fluctuation radial profiles in a single plasma shot [10,11]. Moreover, we have observed the potential and its fluctuation by using the gold neutral beam prove system (GNBP) [9]. We can observe the density and potential fluctuation when the axial confinement potential formation during the application of ECH in a single plasma shot. We observed the suppressions of density fluctuations by the potential formation during ECH. The density and potential fluctuations are observed by using the multi-channel interferometer and GNBP, respectively. Then, we can study more detail about plasma confinement during the formation of confinement potential produced by ECH.

In this paper, we show the phase differences between radial positions of electron densities for the first time, in order to study the direction of the fluctuation propagation. Moreover, we show the results of particle flux analysis by using the GNBP during the formation of the confinement potential with the application of ECH.

2. Experimental Apparatus

GAMMA 10 is an effectively axisymmetrized minimum-B anchored tandem mirror with thermal barrier at both end-mirrors (Fig. 1). In Fig. 1, we show the axis on GAMMA 10. Detail of GAMMA 10 is shown in elsewhere [3-11]. The main plasma confined in GAMMA 10 is produced and heated by ion cyclotron range of frequency power (ICH). The potentials are produced by means of ECH at the plug/barrier region.

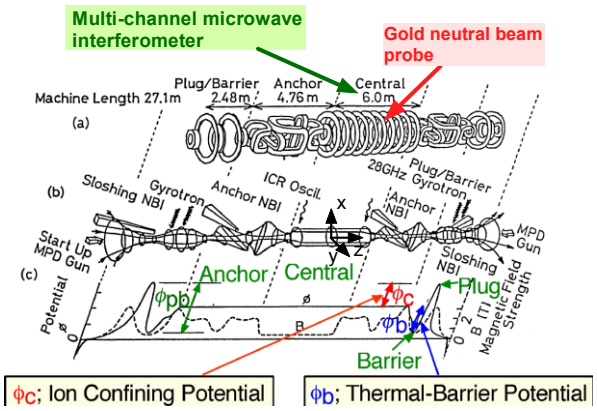

Fig. 1. GAMMA 10 tandem mirror.

author's e-mail: yosikawa@prc.tsukuba.ac.jp

The typical electron density, electron and ion temperatures are about 2 × 10^{18} m^{-3}, 0.1 keV and 5 keV, respectively.

2. 1. Multi-channel Microwave Interferometer

In order to measure radial profiles of both density and density fluctuation, we have constructed the multi-channel microwave interferometer [10,11]. This system can measure electron density and its fluctuation radial profiles in a single plasma shot. It is installed in the central cell mid-plane (z = 0 m). It is designed using Gaussian-beam propagation theory and ray tracing code. Details of this system are shown in elsewhere [10, 11]. A probe microwave beam is injected into the plasma by the transmission horn which is set at the x = 1.15 m and y = –0.10 m though a Teflon lens system from the upper port of the GAMMA 10. The probing locations are y = 0.05 m (ch. 1), 0.01 m (ch. 2), –0.02 m (ch. 3), –0.07 m (ch. 4), –0.10 m (ch. 5), and –0.12 m (ch. 6) at the central horizontal axis of GAMMA 10. The spatial resolution of the system is approximately 3 cm. The line-integrated electron density of each position is calculated numerically. The phase change between the probe and the reference beams is given by the electron density. The Abel inversion technique is used for obtaining the electron density radial profile. Then we can obtain the time dependent radial electron density profiles only by using the multi-channel interferometer in a single plasma shot. We can obtain the temporal electron density on each radial position, $n_e(r,t)$. Normalized electron density Fast-Fourier-Transformed (FFT) frequency spectra are calculated at each radial position.

2. 2. Gold Neutral Beam Probe

We measured the potential and its fluctuations by using a gold neutral beam probe system (GNBP) in the central cell [9]. Details of the GNBP are shown in elsewhere [9]. The plasma density and potential as well as their fluctuations can be measured. Analyzed beam position and beam current in the energy analyzer correspond to the potential and the relative density, respectively. By sweeping the beam trajectory, the system can measure radial profiles of the potential and relative density, and their fluctuations, simultaneously. However, in this experiment, we fixed the beam trajectory in order to measure the potential and density fluctuation at near the center.

3. Density fluctuation measurements

The plasma is produced at 50.5 ms and sustained by ICH. Then barrier-ECH is applied between 159.5 and 204.5 ms to create thermal barrier potential and plug-ECH is applied between 160.5 to 180.5 ms to create confining potentials. Central-ECH is applied between 161.0 to 176.0 ms to increase the electron temperature. Figure 2 shows a time variation of line-integrated density (solid line) measured by the movable interferometer and diamagnetism (dotted line) with the heating sequence. The diamagnetism and electron line density increase with applying ECH. The plasma electron density in the central cell is measured by only using the reconstructed multi-channel microwave interferometer in a single plasma shot. The full width at half maximum of the plasma density before applying ECH is about 0.194 m and that during ECH is about 0.200 m. Then the plasma densities before and during ECH are almost the same. The density on the plasma axis is about 2.5 × 10^{18} m^{-3}. About 20 % of error is included in this measurement, compared with the results of shot-by-shot movable interferometer measuring method.

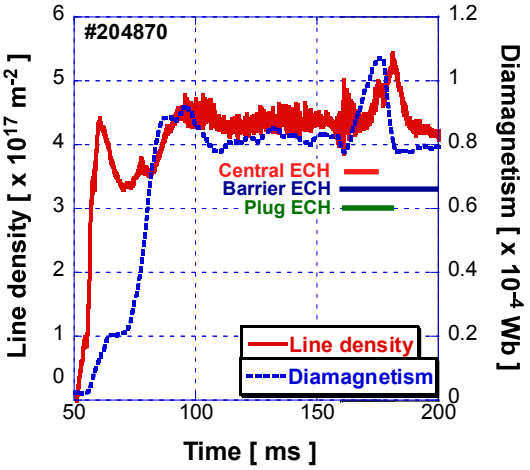

Fig. 2. Temporal behavior of the line density and diamagnetism.

Normalized electron density FFT frequency spectra are displayed in FIG. 3 for each position. FFT spectra of each channel before ECH (hair line, t = 120–122.56 ms) and during ECH (solid line, t = 170–172.56 ms) are shown in FIG. 3 (a) at horizontal position of 0 m, 3 (b) at 0.03 m, 3 (c) at 0.06 m, and 3 (d) at 0.09 m, respectively. It is noticed that the FFT power on each position of plasma densities is suppressed during the application of ECH. The frequency peaks of about 9 kHz are observed before the application of ECH and during application of ECH those frequency peaks are suppressed.

Phase difference near the frequency of 9 kHz between radial position of r = 0 cm and 3 cm, r = 3 cm and 6 cm, r = 6 cm and 9 cm, and r = 9 cm and 12 cm are calculated by cross spectra between them (Fig. 4). In Fig. 4, the closed circle and closed square show the phase

differences at t = 120–122.56 ms and that at t = 170–172.56 ms, respectively. It is confirmed that the

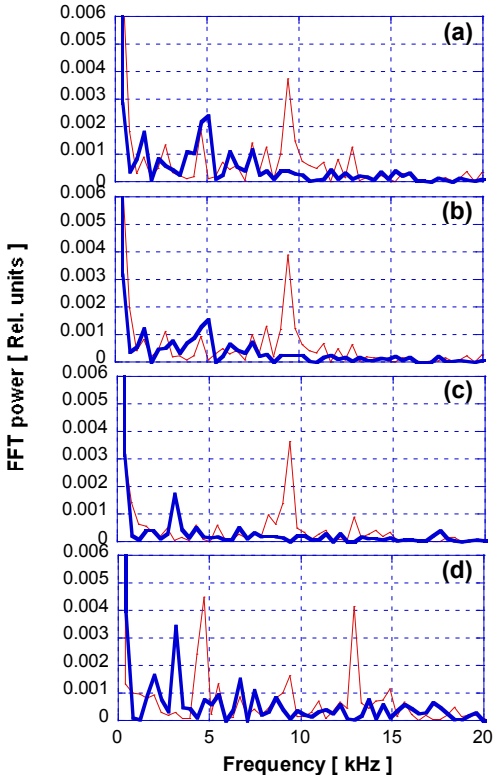

Fig. 3. FFT spectra of each channel before ECH (hair line, t = 120–122.56 ms) and during ECH (solid line, t = 170–172.56 ms) are shown in (a) at horizontal position of 0 m, (b) at 0.03 m, (c) at 0.06 m, and (d) at 0.09 m, respectively.

show the phase differences at t = 120–122.56 ms and that at t = 170–172.56 ms, respectively.

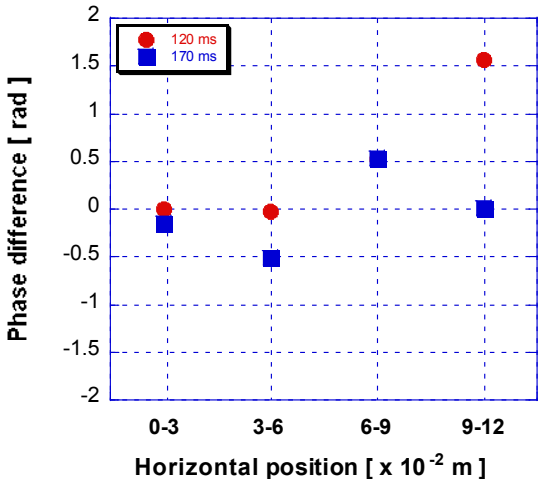

Fig. 4 Phase difference between radial position of r = 0 cm and 3 cm, r = 3 cm and 6 cm, r = 6 cm and 9 cm, and r = 9 cm and 12 cm are calculated by cross spectra between them. The closed circle and closed square show the phase differences before applying ECH and those during the application of ECH, respectively.

phase differences before application of ECH have the direction from the central to the outer on the outer position of plasma compared to that during application of ECH.

4. Density and potential fluctuation measurements

The central-cell potential is raised due to plug potential formation because of improved electron confinement between the central cell and the plug regions in GAMMA 10. Without plug ECH, the potential is relatively low (around 200–300 V). In Fig. 5, we show the FFT spectra of the potential fluctuations measured by using the GNBP system. The peak at the frequency of 9 kHz is observed. When the plug ECH applied (170 ms),

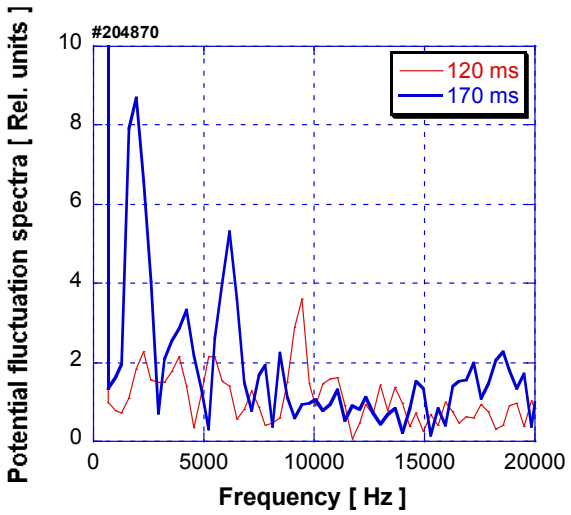

Fig. 5 The FFT spectra of the potential fluctuations measured by using the GNBP system.

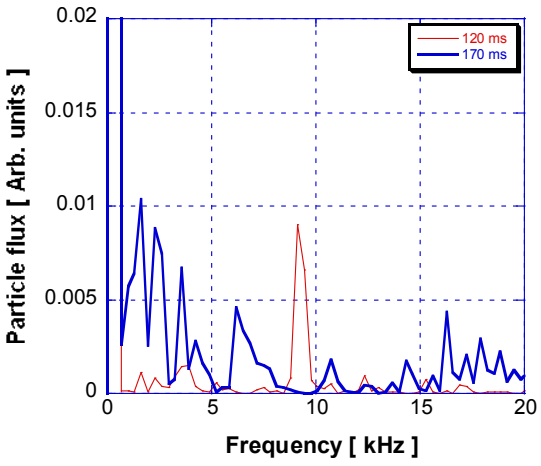

Fig. 6 The particle flux measured at r ~ 2 cm, where the hair line and bold line show the particle flux before application of ECH and that during ECH, respectively.

the decrease of the coherent fluctuation of the 9 kHz peak is observed.

The particle flux was evaluated from the fluctuations of the potential and the density and their phase difference measured by GNBP. In GAMMA 10, the azimuthally propagating electrostatic fluctuations are observed. Radial particle flux for experimental investigation is derived as $\Gamma_p \approx \frac{2}{B}\int_0^\infty k_\theta |\gamma_{n\phi}| \tilde{n}\tilde{\phi} \sin\alpha_{n\phi} d\omega$, where k_θ, $\gamma_{n\phi}$, $\tilde{n}$, $\tilde{\phi}$, $\alpha_{n\phi}$ show the wave number, the coherence between the density and the potential fluctuations, the density and the potential fluctuations, and the phase difference between the density and the potential fluctuations, respectively. We observed the potential and the relative density fluctuation frequencies of about 10 to 12 kHz which correspond to the drift type fluctuation. Figure 6 shows the particle flux measured at r ~ 2 cm, where the hair line and bold line show the particle flux before application of ECH and that during ECH, respectively. The frequency peak about 9 kHz before application of ECH are observed. However, it is decreased during the ECH.

5. Discussion

It is noticed that the FFT power of coherent modes by measurements of the electron density and potential are suppressed during the axially confined potential with application of ECH. The frequency peak of coherent mode about 9 kHz which correspond to the diamagnetic drift is observed before the application of ECH. During the application of ECH the frequency peak of 9 kHz is suppressed. The lower frequency fluctuation, from 2 to 6 kHz, increase is observed during ECH. During ECH, the fluctuation power increase with the production of the higher potential in the central cell.

We carried out the phase difference analysis of the electron density fluctuations between the positions, in order to study the fluctuation propagations for the first time. The study of phase differences between the positions show that the direction of the fluctuation propagation near the frequency of 9 kHz on the period before application of ECH is from the central to the outer in the outer region. The phase difference during the period during the application of ECH is from the outer to the central in the central region of the plasma.

The density and potential fluctuation of coherent mode are suppressed during the formation of the confinement potential with application of ECH. Further studies are required about the density fluctuation suppression mechanisms in the potential confinement during the application of ECH.

The particle fluxes during the application of ECH are analyzed by using GNBP for the first time. The particle flux analysis shows that particle flux induced by the coherent mode fluctuation near the frequency of 9 kHz before application of ECH is larger than that during the application of ECH. However, in this plasma, the lower frequency fluctuation increase during the application of ECH makes the plasma particle confinement worse than that before the application of ECH in the core region.

6. Summary

We studied the density and potential fluctuations during the formation of the confinement potential with application of ECH in GAMMA 10 by using both the multichannel microwave interferometer and GNBP. It is found that low frequency fluctuation, which corresponds to the diamagnetic drift, is suppressed during the formation of confining potential by the application of ECH.

Acknowledgments

The authors would like to thank members of GAMMA 10 group of the University of Tsukuba for their collaboration. This work was partly supported by Ministry of Education, Culture, Sports, Science and Technology, Grant-in-Aid for Scientific Research in Priority Areas, No 16082203.

References

[1] J. C. Forster et al., IEEE Trans. Plasma Sci. **22**, 359 (1994).
[2] D. R. Demers et al., Phys. Plasmas, **8**, 1278 (2004).
[3] A. Mase, J. H. Jeong, A. Itakura, K. Ishii, M. Inutake, and S. Miyoshi, Phys. Rev. Lett., **64**, 2281 (1990).
[4] A. Mase, J. H. Jeong, A. Itakura, K. Ishii, and S. Miyoshi, Rev. Sci. Instrum., **61**, 1247 (1990).
[5] A. Mase, A. Itakura, M. Inutake, K. Ishii, J. H. Jeong, K. Httori, and S. Miyoshi, Nuclear Fusion, **31**, 1725 (1991).
[6] M. Yoshikawa, T. Furukawa, Y. Kubota, K. Sedo, T. Kobayashi, Y. Takemura, K. Ishii, T. Cho, and K. Yatsu, Trans. Fusion Sci. Technol., **43**, 189 (2003).
[7] M. Yoshikawa, Y. Okamoto, E. Kawamori, C. Watabe, Y. Watanabe, T. Furukawa, K. Ikeda, N. Yamaguchi, T. Tamano and K. Yatsu, Trans. Fusion Sci. Technol., **39**, 289 (2001).
[8] M. Yoshikawa, K. Ikeda, Y. Okamoto, E. Kawamori, S. Kobayashi, Y. Nakashima, A. Mase, T. Cho, N. Yamaguchi, T. Tamano, K. Yatsu,

Fusion Technol. **35**, 273 (1999).
[9] Y. Miyata, T. Cho, M. Yoshikawa, Y. Nakashima, M. Hirata, N. Kaidou, H. Kakiuchi, Y. Motegi, S. Goshu, M. Mizuguchi, T. Numakura and J. Kohagura, Plasma Fusion Res. **2**, S1101 (2007).
[10] M. Yoshikawa, Y. Shima, T. Matsumoto, A. Nakahara, N. Yanagi, A. Itakura, H. Hojo, T. Kobayashi, K. Matama, Y. Tatematsu, T. Imai, J. Kohagura, M. Hirata, Y. Nakashima, and T. Cho, Rev. Sci. Instrum. **77**, 10E906 (2006).
[11] M. Yoshikawa, T. Matsumoto, Y. Shima, A. Nakahara, N. Yanagi, A. Itakura, H. Hojo, Y. Kubota, T. Kobayashi, Y. Higashizono, Y. Nakashima, Y. Tatematsu, T. Imai, and T. Cho, Plasma Fusion Res. **2**, S1036 (2007).